A&A 500, L9–L12 (2009)
DOI: 10.1051/0004-6361/200912298

Astronomy & Astrophysics

Letter to the Editor

Possible magnetic field variability during the 6.7 GHz methanol maser flares of G09.62+0.20

W. H. T. Vlemmings[1], S. Goedhart[2], and M. J. Gaylard[2]

[1] Argelander Institute for Astronomy, University of Bonn, Auf dem Hügel 71, 53121 Bonn, Germany
e-mail: wouter@astro.uni-bonn.de
[2] Hartebeesthoek Radio Astronomy Observatory, PO Box 443, Krugersdorp, 1740, South Africa

Received 8 April 2009 / Accepted 29 April 2009

ABSTRACT

Context. Polarization of maser emission contains unique information on the magnetic field in the densest regions of massive star formation.
Aims. Magnetic field induced Zeeman-splitting has been measured for the strongest known 6.7 GHz methanol maser, which arises in the massive star-forming region G09.62+0.20. This maser is one of a handful of periodically flaring methanol masers. Magnetic field measurements can possibly provide insights into the elusive mechanism responsible for this periodicity.
Methods. The 100-m Effelsberg telescope was used to monitor the 6.7 GHz methanol masers of G09.62+0.20, in weekly intervals, for just over a two-month period during which one of the maser flares occurred.
Results. With the exception of a two-week period during the peak of the maser flare, we measure a constant magnetic field of $B_{\|} \approx 11 \pm 2$ mG in the two strongest maser components of G09.62+0.20 that are separated by more than 200 AU. In the two-week period coinciding exactly with the peak of the maser flare of the strongest maser feature, we measure a sharp decrease and possible reversal of the Zeeman-splitting.
Conclusions. While the two phenomena are clearly related, the Zeeman-splitting decrease occurs only close to the flare maximum. Intrinsic magnetic field variability is thus unlikely to be the reason for the maser variability. The exact cause of both variabilities is still unclear, but it could be related to either background amplification of polarized emission or the presence of a massive protostar with a close-by companion. However, the variability in the splitting between the right- and left-circular polarizations could also be caused by non-Zeeman effects related to the radiative transfer of polarized maser emission. In this case we can place limits on the magnetic field orientation and the maser saturation level.

Key words. masers – polarization – magnetic fields – stars: formation – stars: individual: G09.62+0.20

1. Introduction

Polarization observations of astrophysical masers provide important insights into the magnetic field properties of, among others, the dense regions surrounding massive protostars (e.g., Vlemmings 2007, and references therein). In these regions, magnetic fields may play an crucial role in, e.g., suppressing fragmentation, altering feedback processes and stabilizing accretion disks. Linear polarization observations of maser emission can reveal the magnetic field morphology, while observations of the circular polarization, generated by Zeeman-splitting, can be used to measure the line-of-sight magnetic field strength. For the non-paramagnetic molecules, in particular, SiO, H_2O and methanol, maser polarization also depends on intrinsic maser properties that determine the maser saturation level, such as brightness temperature, beaming angle, and the rate of maser-stimulated emission. Thus, polarization observations can, in addition to the magnetic field strength and structure, also provide constraints on maser properties that are otherwise hard to determine (e.g. Vlemmings et al. 2006). Circular polarization or Zeeman-splitting observations have focused mostly on OH and H_2O masers (e.g., Hutawarakorn & Cohen 1999; Sarma et al. 2001; Bartkiewicz et al. 2005; Vlemmings et al. 2006). However, recent observations have revealed significant Zeeman-splitting of the 6.7 GHz $5_1-6_0A^+$ methanol transition (Vlemmings 2008, hereafter V08) in a sample of 17 out of 24 of the brightest northern methanol maser sources, indicating an average magnetic field strength in the maser region of $|B| \sim 20$ mG.

The massive star-forming region G09.62+0.20 harbors the strongest known maser at 6.7 GHz. This maser, and its 12.2 GHz counterpart, undergoes periodic flares with a period of 244 days (e.g., Goedhart et al. 2003, 2004). At the height of its flare, the 6.7 GHz maser has been seen to reach a peak flux density of over 7000 Jy beam^{-1}. There is a time-delay of ~25 days between the flare in the strongest 6.7 GHz feature (hereafter the *main* feature) at ~1.2 km s^{-1} and the *secondary* feature at ~ -0.1 km s^{-1}, which also displays a different flare profile. The origin of the periodic behavior, however, is still unclear. The G09.62+0.20 star-forming region consists of a complex of HII regions at various evolutionary stages. Its 6.7 GHz methanol masers have been mapped with the ATCA by Phillips et al. (1998), and the strongest features are shown to be associated with the hypercompact HII region labeled E by Garay et al. (1993). This region is speculated to be excited by a B0 star (Hofner et al. 1996). VLBA observations of the 12.2 GHz masers during the course of a flare (Goedhart et al. 2005) indicate that the maser regions simply brighten in intensity, with no change in morphology, implying that the cause of the flare originates outside the maser region. It has been previously speculated that the periodicity could originate in either the background HII region, or an infrared pump

source. The monitoring observations presented here were initiated because of the detection of a possible magnetic field reversal between the main ($B_{\parallel} \approx -3$ mG) and secondary ($B_{\parallel} \approx 9$ mG) maser features in V08.

2. Observations and error analysis

The 6668.519 MHz ($5_1-6_0A^+$) methanol maser line of the massive star-forming region G09.62+0.20 was monitored weekly over a period of slightly more than 2 months (11 observing runs between 2008 June 14 and August 20) using the 5 cm primary-focus receiver of the 100-m Effelsberg[1] telescope. The observing dates were chosen to encompass the expected flare events of the main and secondary variable maser features. Unfortunately, a setup problem ensured that data acquired during two observing sessions (June 14 and July 31) were unusable. In addition to G09.62+0.20, we observed G23.01-0.41 as a consistency check. As in previous Effelsberg methanol maser Zeeman-splitting observations (V08), the data were taken in position-switch mode with a 2-min cycle time. Data were collected using the fast Fourier transform spectrometer using two spectral windows, corresponding to the right- and left-circular polarizations (RCP and LCP). The spectral windows of 20 MHz were divided into 16 384 spectral channels, resulting in a ~0.055 km s^{-1} channel spacing, and centered on the local standard of rest (LSR) source velocities. The data were reduced as described in V08, with amplitude calibration performed on 3C 286. The spectrum of G09.62+0.20 for two Effelsberg observational epochs is shown in Fig. 1, along with the circular polarization spectrum for one of the epochs. As seen in the figure, the shape of each maser feature is identical at each epoch. However, the velocity of the maser peak of the main feature is offset in a similar way for both RCP and LCP by up to ~10 m s^{-1}. This is probably caused by a delay of the flare of weaker maser features in the wings of the main feature (Goedhart et al., in prep.).

The target sources G09.62+0.20 and G23.01-0.41 were observed for 10 and 6 min respectively. Because of the changing observing conditions, the rms noise levels varied over the different monitoring sessions. Additionally, the LCP rms noise level was between 50% and 300% higher than the RCP rms noise level. The LCP rms noise, which varied for the 10 min observations of G09.62+0.20 between 100 and 350 mJy, was thus the limiting factor to our Zeeman-splitting determinations. Unfortunately, since the rms noise level was a factor of ~2 higher than that in the V08 observations, we were only able to detect significant Zeeman-splitting in our consistency check source G23.01-0.41 at 4 of the epochs. Within the errors, these epochs were consistent with the V08 observations.

Synchronous observations of G09.62+0.20, as part of a program to monitor the variable methanol maser sources (Goedhart et al. 2005), were carried out using the 26 m telescope at Hartebeesthoek Radio Astronomy Observatory (HartRAO). Full sampling of the flare was not possible because of scheduling constraints. Flux calibrations were done using continuum drift scans across Hydra A and 3C 123 and a further check was made using the methanol maser G351.42+0.64 as a comparison source. Comparison with the HartRAO measurements enabled us to estimate that the absolute flux errors are less than 10%.

Since our observations were aimed at detecting possible small variabilities in the Zeeman-splitting, we performed an additional analysis of the channel rms noise in the spectrum of G09.62+0.20. To determine the increase in channel rms noise as a function of maser flux, we used the 5 individual 2-min scans of two of the epochs to determine the channel rms in those channels containing significant maser emission. The individual maser spectra were normalized to the peak flux of the combined scans to minimize the effect of intrinsic maser variability. We then calculated $\Delta_i = \mathrm{rms}_i/\sigma$ for each channel i, where σ is the rms noise value for the emission-free channels. Figure 2 shows Δ as a function of the maser flux in each of the channels with $>5\sigma$ maser emission. For all of the maser features, we found that, with one exception, Δ stays approximately constant within a factor of ~3 up to a maser flux of ~50 Jy beam^{-1}, after which it increases with $\Delta \propto (\mathrm{Flux})^{0.9}$. During the first epoch, only the maser feature at $V_{\mathrm{LSR}} = 5.4$ km s^{-1} did not follow this relation and already deviated from the expected rms noise level when its flux became >20 Jy beam^{-1}. Since this did not occur during the last epoch, this is possibly due to weak narrowband interference. Since the noise characteristic is similar for both polarizations and all epochs, the rms error increase is unlikely to be caused by receiver saturation and would be unable to cause a systematic shift between RCP and LCP. However, the analysis does imply that the errors in the Zeeman-splitting determination in V08 should be increased. For the majority of the masers in V08, this increase is less than a factor of ~5. However, for the masers of G09.62+0.20, the errors need to be increased by a factor of 40 and 8 for the main and secondary maser features, respectively.

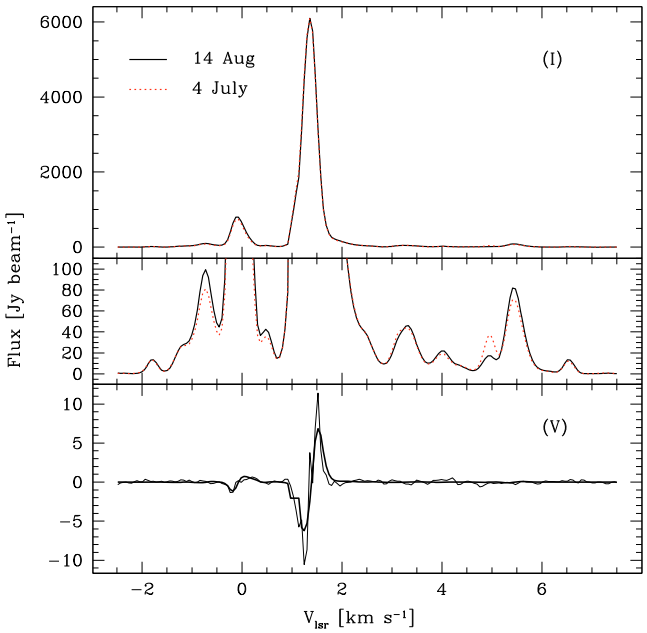

Fig. 1. The 6.7 GHz methanol maser total intensity (I) spectrum of G09.62+0.20 for two observing epochs. The peak flux at July 4 is scaled to the flux at Aug. 14 2008 (*top*). *The middle panel* highlights the many weaker maser features of this region. *The bottom panel* shows the circular polarization spectrum (V) for the observations at Aug. 14 2008. The thick solid line is the best fit fractional total intensity derivative.

3. Variability in the RCP-LCP frequency splitting

3.1. The case of G09.62+0.20

We determined the Zeeman-splitting of the two brightest 6.7 GHz methanol maser features of G09.62+0.20 using the RCP-LCP cross-correlation method as described in V08.

[1] The 100-m telescope at Effelsberg is operated by the Max-Planck-Institut für Radioastronomie (MPIfR) on behalf of the Max-Planck-Gesellschaft (MPG).

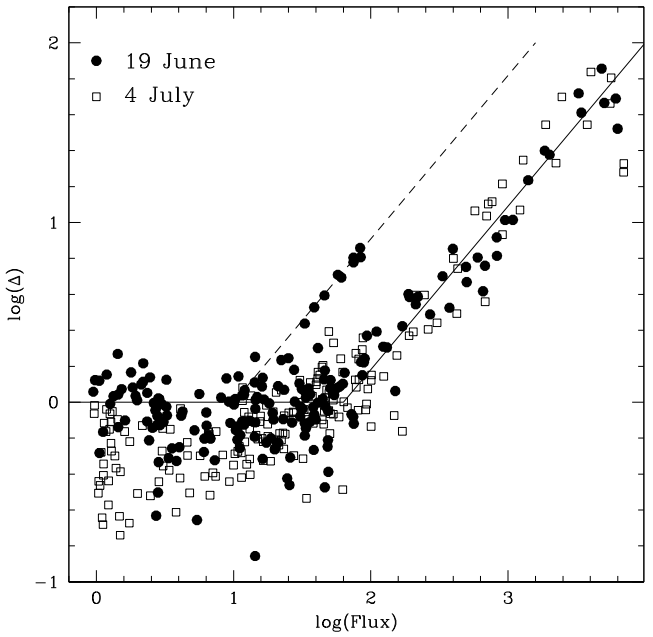

Fig. 2. The ratio Δ of the true to predicted channel rms noise as a function of channel flux for two epochs. The solid line indicates a two-component description of the rms noise increase due to dynamic range limits of the spectrometer. The dashed line indicates the anomalous increased rms noise for the maser features at V_{LSR} = 5.4 km s^{-1} seen in the first epoch.

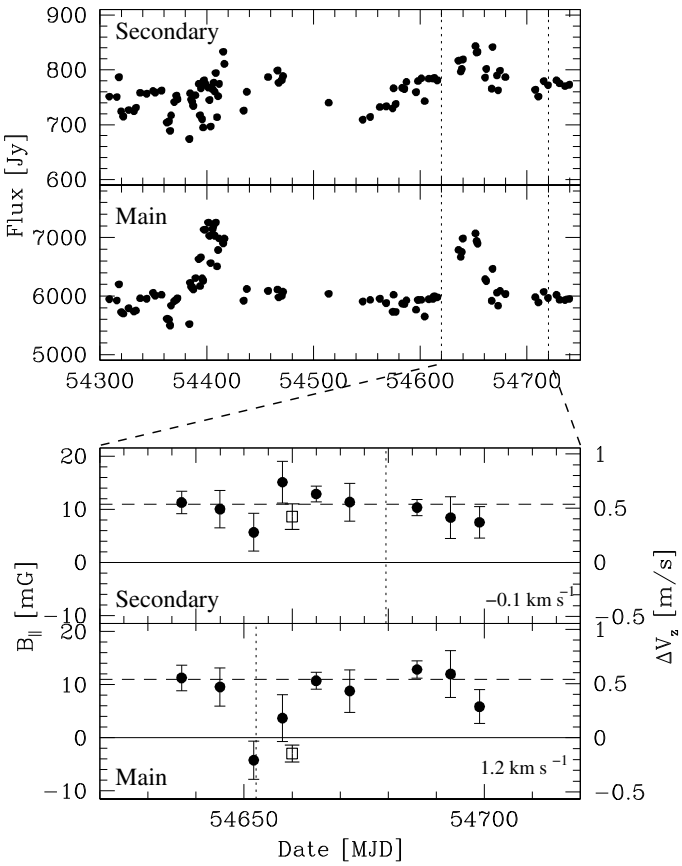

Fig. 3. (*Bottom panels*) The Zeeman-splitting ΔV_Z (in m s^{-1}) and derived line-of-sight magnetic field strength $B_{\|}$ (in mG) for the two strongest 6.7 GHz methanol maser features of G09.62+0.20 at the 9 successful monitoring epochs (filled dots). The previous observations of Nov. 11th 2007 (open square; V08) has been folded into the new observations. The vertical short-dashed lines indicate the predicted date of the emission peak. The horizontal dashed lines indicate the weighted average magnetic field strength (see text). (*Top panels*) HartRAO telescope observations of the two maser features for two flaring periods. The period of the Effelsberg observations is indicated by the vertical short-dashed lines.

Figure 3 shows the line-of-sight magnetic field strength $B_{\|}$ for the two maser features at each epoch derived from the Zeeman-splitting ΔV_Z, using 0.049 km s^{-1} G^{-1} as the best estimate of the Zeeman-splitting coefficient. In addition to the monitoring epochs, the figure also includes the folded-in observations presented in V08. We found that the line-of-sight magnetic field strength in the secondary maser feature is stable during the observations with an error-weighted average magnetic field of $B_{\|}$ = 10.9 ± 2.3 mG. In contrast, the Zeeman-splitting of the main maser feature sharply decreases as the maser flare reaches its peak flux. Monitoring at weekly intervals has proven to be too coarse to place strong constraints on the length of the period with decreased ΔV_Z. However, while the typical duration of a flare is up to two months, the decrease in Zeeman-splitting lasts only for an approximate two-week period around the peak of the flare. Determining an error-weighted average magnetic field for the main maser feature using the 7 epochs on either side of the two-week period with decreased Zeeman-splitting, we found $B_{\|}$ = 11.0 ± 2.2 mG. Thus, the magnetic field strength is remarkably similar in both masers, even though both features are separated by more than 200 AU (Goedhart et al. 2005).

Figure 3 thus indicates that when the flare of the main maser feature reaches its peak flux, the Zeeman-splitting decreases significantly and potentially even changes sign. Since the observations of V08 that also revealed a much lower (and possibly reversed) ΔV_Z were taken close to the peak of the previously flaring period, this behavior appears to repeat itself regularly. No significant Zeeman-splitting decrease is seen for the secondary maser feature. The observations with the HartRAO telescope showed that the flare of this feature, while occurring typically approximately 25 days after the flare of the main feature, was much more irregular and reached its peak at about the same time as the main feature. However, throughout the Effelsberg observations its flux variations were only ∼10%, while that of the primary feature was over 20%.

3.2. Possible origin of the observed variability

The cause of the sudden decrease in Zeeman-splitting during the maser flare is unknown. We can confidently exclude instrumental effects as the reason for the decrease in ΔV_Z of the main maser feature for a number of reasons. First of all, no significant corresponding decrease is found for the secondary maser feature at the same epochs. Furthermore, the almost constant Zeeman-splitting measured before and after the peak and the negative Zeeman-splitting found during the maser flare 8 months earlier, confirm the stability of the instrumental setup as well as the robustness of the data reduction and analysis method.

The observed effect is thus probably intrinsic to the source. The measured decrease in ΔV_Z however, starts after the maser flux has already entered the flaring stage. Thus, while the measured Zeeman-splitting variation is related to the maser flare, it is unlikely that the flare itself is caused by changes in the magnetic field. We describe three possible scenarios that could give rise to the observed effect.

Background amplification: since the observed Zeeman-splitting is generated by the average magnetic field throughout the entire maser region, the most straightforward cause of a drop in observed Zeeman-splitting is the superposition of two maser regions with opposite magnetic fields. As described in Boboltz et al. (e.g., 1998), maser flares can often be attributed to the chance alignment of maser regions, when a foreground maser amplifies the emission from a background maser. Alternatively, instead of a maser, the background source could be a strongly polarized continuum source. In this case, polarization of the seed emission can cancel out any circular polarization generated within the maser. However, while this simple model also naturally explains the maser flare, the origin of the observed periodicity remains unclear.

Intrinsic magnetic field variability: a second option is that the observations reveal an actual change in the magnetic field within the maser region. Various mechanisms can produce a change in magnetic field. It has been suggested that the periodic maser flares are caused by changes in the maser pumping resulting from a binary interaction between a massive protostar and companion (Goedhart et al. 2003). Interactions between the magnetospheres of the two companions could cause a periodic behavior of the magnetic field, as has been observed in young low-mass binary systems (e.g., Massi et al. 2008). However, typical magnetic reconnection events do not last long enough to explain the approximate two-week duration of the magnetic field variability. It is also unclear whether the magnetic interaction would be noticeable in the methanol maser region at a distance of several hundred AU from the protostars. Still, an embedded binary will also give rise to other complex interactions besides that of the magnetic field, such as those between possible accretion disks and outflows. These interactions will be imprinted onto the observed magnetic field. Thus, if the observed magnetic field variability is truly due to intrinsic changes of the magnetic field, any possible explanation of the periodic maser flares will also need to take into account the behavior of the magnetic field.

Maser radiative transfer: alternatively, we are observing a combination of Zeeman and non-Zeeman effects, competing while the maser is at its brightest. Non-Zeeman effects were briefly discussed in V08. Specifically both the axis of symmetry for the molecular quantum states rotating when the maser saturates, and the rate of stimulated emission R becoming greater than the Zeeman frequency shift $g\Omega$, bear further investigation. An unfortunate error was introduced in the calculation of $g\Omega$ presented in V08, where the true $g\Omega$ is smaller than presented there. For a typical magnetic field strength B, in the dense maser region, on the order of 10 mG, $g\Omega \approx 13$ s^{-1}, approximately three times larger than the rate of stimulated emission $R \sim 4$ s^{-1} for the most saturated 6.7 GHz methanol masers with a maser brightness temperature $T_b \sim 10^{12}$ K sr. This assumes a typical maser beaming angle $\Delta\Omega = 10^{-2}$ sr, which decreases rapidly when the maser saturates. Thus, for most typical methanol masers with T_b on the order of a few times 10^{10} K, we have $R < 0.1$ s$^{-1} \ll g\Omega$ and little or no intensity-dependent polarization is generated. This is supported by the lack of a relation between maser intensity and Zeeman-splitting in V08. However, the brightest masers of G09.62+0.20 could have an R that approaches or even becomes larger than $g\Omega$, raising the possibility of intensity-dependent circular polarization mimicking the Zeeman-splitting between the RCP and LCP spectra. The generation of circular polarization due to this effect has been investigated for a $J = 2{-}1$ transition by Nedoluha & Watson (1990). Although the effect is likely smaller for the transition of the 6.7 GHz methanol masers involving higher angular momentum states, the sign of the circular polarization, and consequently the sign of the splitting between RCP and LCP, is found to be the opposite of that generated by the regular Zeeman effect when the angle between the magnetic field and the maser line of sight θ obeys $\sin^2\theta < 2/3$. Observationally, this implies that with increasing maser brightness temperature and consequently R, the observed splitting between RCP and LCP spectra decreases. Since the average Zeeman-splitting of the two maser features, with fluxes that differ by an order of magnitude, are identical, the non-Zeeman effect apparently only becomes important when the flare reaches its maximum flux. This indicates the masers of G09.62+0.20 approach complete saturation at the peak of the flare. It will be possible to test the hypothesis of the non-Zeeman interpretation of the observed splitting variability by simultaneously observing the maser linear polarization, because similar considerations predict an intensity dependence of fractional linear polarization and polarization angle.

4. Conclusions

We have presented Effelsberg 100-m telescope monitoring observations of the RCP-LCP frequency splitting of periodically flaring 6.7 GHz methanol masers in the massive star-forming region G09.62+0.20. A significant decrease in Zeeman-splitting and thus possibly magnetic field strength is detected for the strongest maser feature during a two-week period surrounding the flare maximum. Besides this decrease, a remarkable constant $B_{\|}$ of ~11 mG is detected for the two brightest maser features separated by over 200 AU. The cause of this decrease in measured Zeeman-splitting is still unclear but is either related to the mechanism causing the periodic maser flaring or a result of a non-Zeeman effect when the maser saturation level becomes significant.

Thus, G09.62+9.20, with the relative predictability of the flares, varying levels of intensities amongst maser features, and correlated variability in RCP-LCP frequency splitting, is an ideal natural laboratory for testing theories related to both massive star formation and maser physics.

Acknowledgements. W.V. acknowledges support by the *Deutsche Forschungsgemeinschaft* through the Emmy Noether Research grant VL 61/3-1. W.V. also thanks Alex Lazarian and Bill Watson for kindly answering a number of his questions.

References

Bartkiewicz, A., Szymczak, M., Cohen, R. J., & Richards, A. M. S. 2005, MNRAS, 361, 623
Boboltz, D. A., Simonetti, J. H., Dennison, B., Diamond, P. J., & Uphoff, J. A. 1998, ApJ, 509, 256
Garay, G., Rodriguez, L. F., Moran, J. M., & Churchwell, E. 1993, ApJ, 418, 368
Goedhart, S., Gaylard, M. J., & van der Walt, D. J. 2003, MNRAS, 339, L33
Goedhart, S., Gaylard, M. J., & van der Walt, D. J. 2004, MNRAS, 355, 553
Goedhart, S., Minier, V., Gaylard, M. J., & van der Walt, D. J. 2005, MNRAS, 356, 839
Hofner, P., Kurtz, S., Churchwell, E., Walmsley, C. M., & Cesaroni, R. 1996, ApJ, 460, 359
Hutawarakorn, B., & Cohen, R. J. 1999, MNRAS, 303, 845
Massi, M., Ros, E., Menten, K. M., et al. 2008, A&A, 480, 489
Nedoluha, G. E., & Watson, W. D. 1990, ApJ, 361, L53
Phillips, C. J., Norris, R. P., Ellingsen, S. P., & McCulloch, P. M. 1998, MNRAS, 300, 1131
Sarma, A. P., Troland, T. H., & Romney, J. D. 2001, ApJ, 554, L217
Vlemmings, W. H. T. 2007, in IAU Symp., 242, 37
Vlemmings, W. H. T. 2008, A&A, 484, 773
Vlemmings, W. H. T., Diamond, P. J., van Langevelde, H. J., & Torrelles, J. M. 2006, A&A, 448, 597